ISSN: 0975-766X
CODEN: IJPTFI
Available Online through ***Research Article***
www.ijptonline.com

DETERMINATION OF SAPPHIRE SINGLE CRYSTAL GROWTH DYNAMICS BASED ON VISUAL INFORMATION

Alexander Vladimirovich Belousov*, Iurii Alekseevich Koshlich, Artyom Grigorevich Grebenik
Belgorod State Technological University named after V.G. Shukhov,
Russia, 308012, Belgorod, Kostyukova, 46.

Received on 06-08-2016 *Accepted on 10-09-2016*

Abstract

The paper formalized algorithm analysis of the dynamics of growth of a crystal sapphire in the production of method Kyropoulos. It is proposed a method of estimating the rate of growth of single crystals on the basis of analysis of the distribution of the radiation intensity on trace rays. The data obtained can be used to obtain crystals of visual patterns. Focuses on the mathematical treatment of radiometric images obtained in the crucible growth installation produced by Tech Sapphire Ltd. Obtaining of operation visual information about temperature distribution inside the crucible is a key point and it's reduced to getting a visual picture using CCD-camera. Sobel operator is used to present the image in more readable form for personal computer. Favor of data smoothing based on Gaussian function.

Keywords: Control system, automated seeding, sapphire, Kyropoulos method, Sobel operator, Gaussian distribution, radiometric image.

1. Introduction. Field of sapphire application is determined by the following properties: mechanical strength, chemical and biological inertness, high transparency and non-conductivity [1, 2].

Main applications of synthetic sapphire:

1. Microelectronics (substrate for semiconductor device
2. Optoelectronics (substrates for light-emitting diodes (LEDs) used for general illumination, screens, annunciators, advertising surfaces, etc.).
3. Optics and Instrumentation (lenses, windows and fibers for optical devices, including cameras, military purpose devices).
4. Medicine (optical windows of laser devices, optical fibers, scalpels and dentures: bones, tooth implants, lenses and etc.).

5. Watch industry (watch glasses and parts of mechanism.)
6. Industrial machinery (parts requiring high strength and resistance to aggressive environments such as pipes, crucibles, funnels, capillaries, chemical vessels and etc.).
7. Automobile manufacturing (protective glass lamps, lights and signals).
8. Aviation and Aerospace (portholes of aircraft and spacecraft, radomes of missiles and aircraft).

Most of world synthetic sapphire market is the substrates for chips and LEDs. Technology of sapphire crystals growing have been developed in the 60s (and the first samples were obtained in the beginning of the century XX). Now are used several methods (Verneuil, Kyropoulos, Czochralski and horizontal directional solidification) [3-5]. However, each manufacturer making their own changes in design of sapphire crystal growth stations (growth machines) as well as in the technology. The significance of these changes is obtaining larger crystals of better quality. The seeding process is performed manually by the operator because of insufficient theoretical development of Kyropoulos method and not enough accurate (in terms of measurement) hardware components of measuring instruments and lack of a formalized algorithm. The result depends on the qualification and specific qualities of the operator, human factor.

2. Procedure

A software and hardware complex is represented to solve the problem, which should greatly increase automation level of production process by means of formalized seeding algorithm based on visual information. To achieve the goal it's necessary to solve some local problems, such as development of processing algorithm of radiometric measurements in the crucible of growth station, development of algorithm and software to determine the dynamics of crystal growth, development of imaging subsystem of seeding process in real time and development of mathematical model of heat and mass transfer of sapphire crystallization when using Kyropoulos method.

At the same time it's important not only clear visual picture of the process, but also possibility of metric data obtaining, particularly the growth rate and size of crystal neckД growth steps. This data is important when setting growth equipment for crystallization and automatic generation of the crystal growth program for each station. This development has been successfully tested on Techsapphire growth stations.

Obtaining of operation visual information about temperature distribution inside the crucible is a key point and it's reduced to getting a visual picture using Charge-Coupled Device (CCD) camera with properly chosen optics and filter. Using libraries provided by manufacturer for developing applications it's available to get radiometric

measurements (as image, each pixel contains information about the color temperature of the melt surface i. e. digital level (Figure **1**).) [6-10].

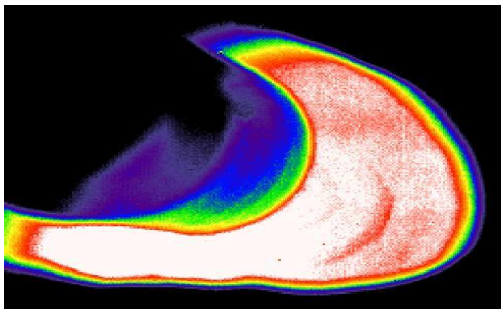

Fig. (1). Radiometric measurements in the growth station crucible.

(The picture is obtained during the growth process on Techsapphire growth station).

This is exactly array data where each coordinate contains emission intensity information.

Sobel operator is used to present the image in more readable form for personal computer (pc) which uses 3x3 pixel area of image. Sobel operator is more inaccurate approximation of the gradient image, but it has sufficient quality to be practical in many applications.

For image processing pixel neighborhood 3x3 is used (Figure **2**).

z_1	z_2	z_3
z_4	f(x,y)	z_6
z_7	z_8	z_9

Fig. (2). Processing pixel neighborhood.

Determination of the gradient is to use the weighting coefficient for average elements:

$$G_x = \frac{\partial f(x,y)}{\partial x} = (z_7 + 2z_8 + z_9) - (z_1 + 2z_2 + z_3)$$

and

$$G_y = \frac{\partial f(x,y)}{\partial y} = (z_3 + 2z_6 + z_9) - (z_1 + 2z_4 + z_7)$$

This increased value is used to reduce the smoothing effect by more weight of middle points. Masks used by Sobel operator are showed in Figure **3**.

-1	-2	-1
0	0	0
1	2	1

-1	0	1
-2	0	2
-1	0	1

Fig. (3). Masks of Sobel operator.

The above masks are used for Gx and Gy gradient components. To calculate the the gradient these components must be used together:

$$f(x,y) = \sqrt{G_x^2 + G_y^2}$$

But for practical application enough the calculating:

$$\nabla f(x,y) \approx |G_x| + |G_y|$$

As processing result will be image shown in Figure **4**.

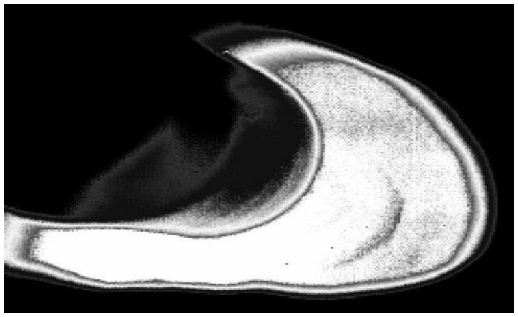

Fig. (4). The processed image.

The dynamics of crystal growth is determined by the distance between step of the crystal neck growth and its boundary, which can be determined by calculating the global extreme points of intensity distributions. Using developed algorithm support for receiving and processing of crystal state images during the seeding with the help of libraries provided by manufacturer for developing applications, it's available to get radiometric measurements (as image, each pixel contains information about the color temperature of the melt surface i. e. digital level (Figure **5**)) [10, 11].

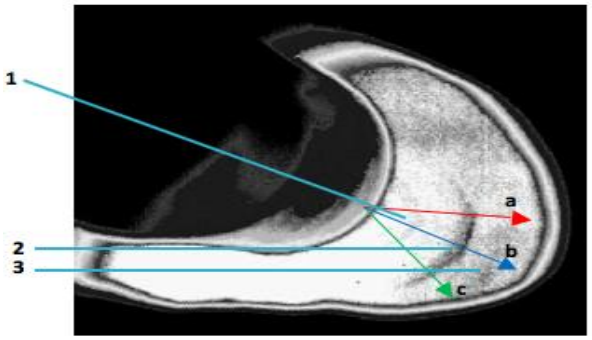

Fig. (5). Processed radiometric measurements in the crucible of the growth station (1 - edge of the seed crystal, 2 - step of the crystal neck growth, 3 - edge of the single crystal; on the picture provisionally designated as tracing rays a - red, b - blue, c – green).

The dynamics of crystal growth is determined by the distance between step of the crystal neck growth 2 and its boundary 2, which can be determined by calculating the local extreme points of intensity distributions of tracing rays (Figure-**6**).

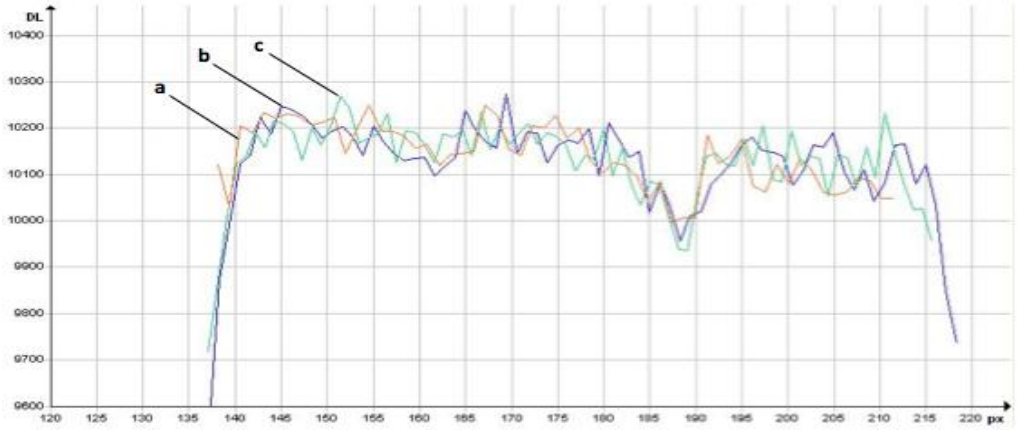

Fig. (6). The intensity distribution level (DL) on the trace rays (trend color on the graph corresponds to the intensity distribution on the trace ray of the corresponding color in Figure 2).

According to developed algorithmic support of image acquisition and processing of the single crystal state during seeding stage, image capture occurs at every turn of seed holder. Search of local extremes of intensity distribution on the tracer ray is complicated by luminance noises (Figure **7**). Therefore, signal smoothing is performed for processing of received distributions.

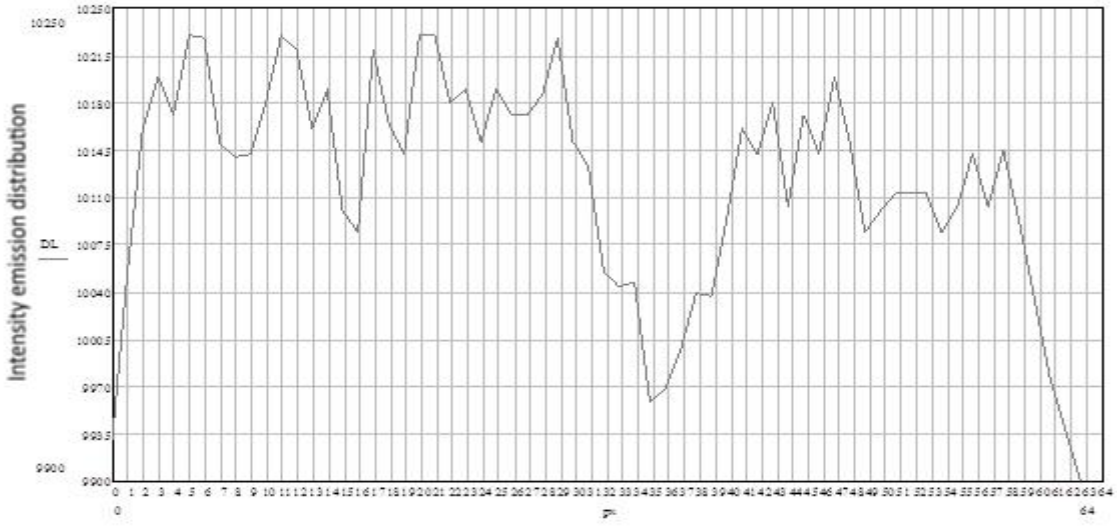

Fig. (7). Intensity emission distribution on the tracer ray (DL is level of intensity in arbitrary units of digital level).

When analyzing the signal filtering methods [3, 12], the choice was made in favor of data smoothing based on Gaussian function (1), since this smoothing suppresses the noise by supporting the requirement: the points "should be similar" to their neighbors. Reducing the weighting factors for distant points, you can be sure that this requirement will not be so tough for them.

$$K(t) = \frac{1}{\sqrt{2\pi}\cdot\sigma} \cdot e^{-\left(\frac{t^2}{2\cdot\sigma^2}\right)}, \qquad (1)$$

where σ - the standard deviation of the Gaussian distribution.

$$DH_i = \frac{\sum_{j=0}^{m-1} K\left(\frac{px_i - DH_j}{b}\right) DH_j}{\sum_{j=0}^{m-1} K\left(\frac{px_i - px_j}{b}\right)}, \quad (2)$$

where b - filter aperture, m - the number of points.

If σ is very small (for example, σ << 1), the smoothing will give insignificant result because the weighting coefficients of all pixels located not in the center will be very small.

For more σ neighboring pixels have more weighting coefficients using the weighted average, it means that the average value is seek harmonization with neighbors, it's good estimate of the pixel value, and by blurring most of the noise will disappear.

The increase of σ will lead to disappearance of signal major part along with the noise.

Smoothed with Gaussian function with σ = 0,37 and b = 3 intensity distribution on trace beam is shown in Figure **8**.

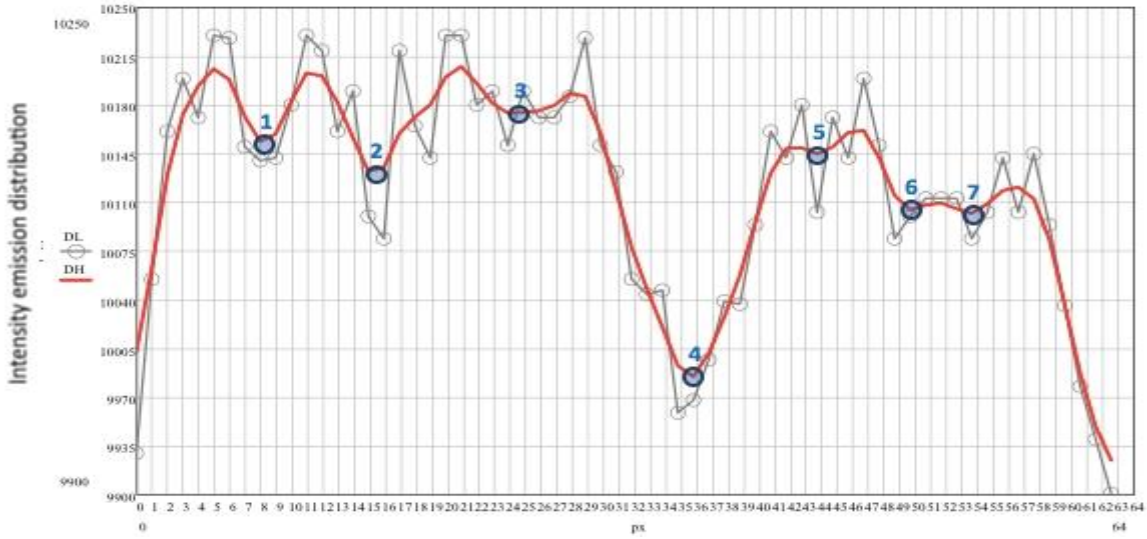

Fig. (8). The intensity distribution smoothed on the basis of Gaussian function (DL is intensity level in conditional units of digital level, DH is smoothed intensity distribution, 1-7 are local minima points of DH distribution).

But operating with smoothed DH curve for the extrema determination is meaningless, because the required minimum distribution values 2 and 4, which coordinates correspond to the edge of crystal neck growth (by plane through tracing ray) will include extra points (1, 4, 5, 7, 13), the which extremes are caused by non-uniformity of temperature distribution and luminance noise.

Getting values of global extrema with sufficient accuracy is possible with the approximation of the intensity distribution. Polynomial approximation on the basis of the least squares method was chosen as an approximation method. If number of neck growth steps increase, it's necessary to change the degree of the approximating polynomial.

$$DA(px) = \sum_{i=0}^{n} C_i px^{n-i}, \quad (3)$$

where n is the degree of the polynomial.

Decision of the task is the vector that minimizes the deviation of E (x) (4) - the total error of approximation.

$$E = \sum_{j=0}^{m-1} \left(DH(px_j) - \sum_{i=0}^{n} C_i px_j^{n-i} \right)^2, \quad (4)$$

where m is the number of distribution points.

Finding the coefficients of approximating polynomial is reduced to solving a system of n equations (5).

$$\frac{\partial E}{\partial C_i} = 0, \quad (5)$$

Algorithm is selected as a numerical method for solving of algebraic equations using singular value decomposition (SVD), allowing to solve ill-conditioned problems and even problems with a singular system of basis functions.

Regarding the present case, when primary and growing step of neck growth is in the camera view, ie function must have two minimums, with sufficient accuracy the distribution can be approximated by polynomial of the seventh degree (n = 7) (Figure **9**).

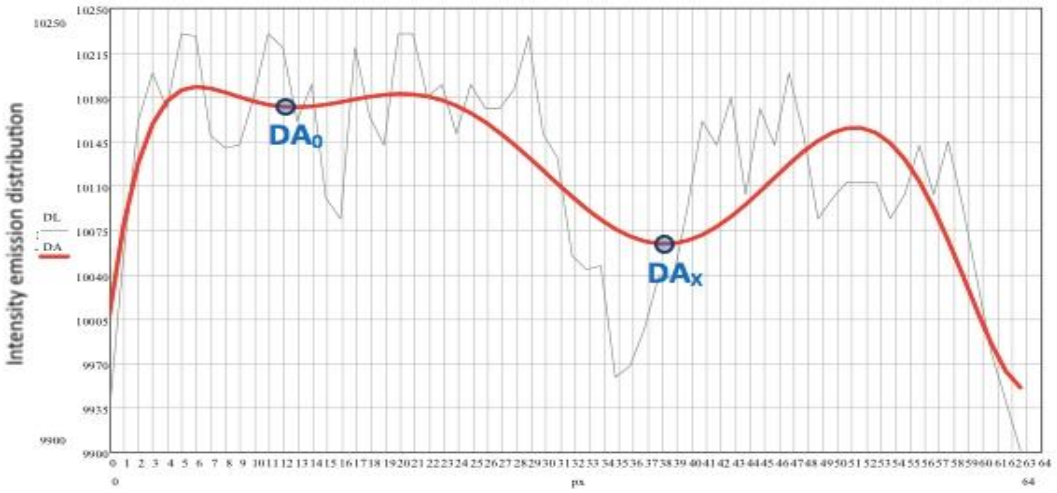

Fig. (9). The polynomial approximation of the intensity distribution smoothed on the basis of the Gaussian function (DL is intensity level in conditional units of digital level, DA is approximating polynomial.)

The value of d_0 in which approximates polynomial DA takes the extreme value DA_0 corresponds to the distance from center of initial seed crystal contact the melt up to the first step of crystal neck growth, and the desired value of d_x, where the approximating polynomial DA takes the extreme value DA_x is Distance to the phase change boundary, dynamics definition which changes correspond to the definition of the crystal growth dynamics to the corresponding front.

For a two-dimensional visual model of the crystal (Figure **10**) in a plane perpendicular to seed holder of growth

station, it's necessary to move from Cartesian to polar coordinates followed by distance determination d_0, d_1,…, d_x.

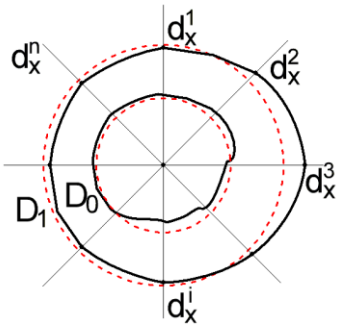

Fig .(10). Two-dimensional crystal model.

3. Software Implementation. During the seeding process it's necessary to form a control signal depending on solidification front dynamics in an effort to evenly crystal growth in all directions.

The intensity distribution along the trace ray to be found by processing of frame of seeding process by OpenCV library. OpenCV (Open Source Computer Vision Library, a library of computer vision of open source) is a library of algorithms for computer vision, image processing and numerical algorithms for general purpose with open source software. Implemented in C / C + +, also being developed for Python, Java, Ruby, Matlab, and other languages. It may be used freely for academic and commercial purposes and be distributed under Berkley Software Distribution license (BSD license).

The software implementation is based on a Python language using library of SciPy modules. This library is necessary to ensure a satisfactory rate of algorithm execution: resource-intensive library functions implemented in C + + language and represents machine code invoked by wrapper functions of the Python language interpreter. Thus, the mathematical operations associated with the data manipulation in cycles are performed ten times faster than when implemented by standard language means.

Obtained one-dimensional array function values of the radiation intensity distribution on the trace rays is passed to the gsmooth function, which returns an array of values of the smoothed distribution function. Gsmooth function uses Gaussian kernel to to calculate local weighted averages of the initial vector. The fragment gsmooth forming an array of smoothed functions is given below:

```
if sigma is not None:
    isigma = numpy.ceil(sigma/dt)
    lenG = 6*isigma
    G = scipy.signal.gaussian(lenG, isigma)
```

```
sdf = scipy.signal.convolve(sdf, G)

sdf = sdf[lenG/2:-(lenG/2-1)]
```

On the basis of the obtained values polynomial approximation of smoothed functions by least squares is performed. Searching C_i coefficients of the approximating polynomial of distribution functions performed by lasolver procedure, solves a system of n equations by the method of singular value decomposition by means of the open NumPy library.

```
def lasolver(A, b):
# The initial system of equations – Ax=b
# A singular matrix value decomposition of A system of equations
U,s,V = linalg.svd(A)
# c = U^t*b
c = dot(U.T,b)
# w = V^t*c
w = linalg.solve(diag(s),c)
# x = V*w – desired coefficient vector of polynomial
X = dot(V.T,w)
return x
```

Lasolver function produces a singular value decomposition of the coefficient matrix of the system of equations with help svd function, relying on the solvers of the library with LAPACK open source.

```
def svd(a, full_matrices=1, compute_uv=1):
    a, wrap = _makearray(a)
    _assertRank2(a)
    _assertNonEmpty(a)
    m, n = a.shape
    t, result_t = _commonType(a)
    real_t = _linalgRealType(t)
    a = _fastCopyAndTranspose(t, a)
    a = _to_native_byte_order(a)
    s = zeros((min(n, m),), real_t)
```

```
if compute_uv:
    if full_matrices:
        nu = m
        nvt = n
        option = _A
    else:
        nu = min(n, m)
        nvt = min(n, m)
        option = _S
    u = zeros((nu, m), t)
    vt = zeros((n, nvt), t)
else:
    option = _N
    nu = 1
    nvt = 1
    u = empty((1, 1), t)
    vt = empty((1, 1), t)
iwork = zeros((8*min(m, n),), fortran_int)
if isComplexType(t):
    lapack_routine = lapack_lite.zgesdd
    lrwork = min(m,n)*max(5*min(m,n)+7, 2*max(m,n)+2*min(m,n)+1)
    rwork = zeros((lrwork,), real_t)
    lwork = 1
    work = zeros((lwork,), t)
    results = lapack_routine(option, m, n, a, m, s, u, m, vt, nvt,
                             work, -1, rwork, iwork, 0)
    lwork = int(abs(work[0]))
    work = zeros((lwork,), t)
```

```
    results = lapack_routine(option, m, n, a, m, s, u, m, vt, nvt,
                             work, lwork, rwork, iwork, 0)
  else:
    lapack_routine = lapack_lite.dgesdd
    lwork = 1
    work = zeros((lwork,), t)
    results = lapack_routine(option, m, n, a, m, s, u, m, vt, nvt,
                             work, -1, iwork, 0)
    lwork = int(work[0])
    work = zeros((lwork,), t)
    results = lapack_routine(option, m, n, a, m, s, u, m, vt, nvt,
                             work, lwork, iwork, 0)
  if results['info'] > 0:
    raise LinAlgError, 'SVD did not converge'
  s = s.astype(_realType(result_t))
  if compute_uv:
    u = u.transpose().astype(result_t)
    vt = vt.transpose().astype(result_t)
    return wrap(u), s, wrap(vt)
  else:
    return s
```

Thus searching of approximating polynomial coefficients of the intensity distribution function of given degree. Found coefficients used in the future to search for local extremes of the approximated function by extrema procedure.

```
def extrema(x, max = False, min = True, strict = False, withend = False):
    """
The function returns an array of indices of extreme points in the original one-dimensional array.
"""
# Value calculation of the first derivative.
```

```
from numpy import zeros
    dx = zeros(len(x))
    from numpy import diff
    dx[1:] = diff(x)
    dx[0] = dx[1]
# Filtering Values by sign.
from numpy import sign
    dx = sign(dx)
# The threshold determines the sensitivity of the algorithm.
threshold = 0
    if strict:
    threshold = 1
# Searching of the extremum by the second derivative.
d2x = diff(dx)
    if max and min:
        d2x = abs(d2x)
    elif max:
        d2x = -d2x
    if withend:
        d2x[0] = 2
        d2x[-1] = 2
Screenings of minor fluctuations.
from numpy import nonzero
    ind = nonzero(d2x > threshold)[0]
    return ind
```

The indices obtained as a result of extrema function execution, define desired coordinates of d_o, d_1, … ,d_n minimums of intensity distribution approximate function. On the basis of obtained minimum value two-dimensional visual model of sapphire single crystal during the seeding is building.

4. Conclusion. Thus, the software implementation formalized algorithm will yield a crystallization rate and evaluate the dynamics of growth. The data obtained can be used to obtain crystals of visual patterns. Use of the information in the control systems will significantly increase the degree of automation of technological processes of production of single-crystal sapphire method Kyropoulos. In the process of seeding is necessary to form a control signal depending on the dynamics of the crystallization front, achieving uniform in all directions of the crystal growth.

References

1. Teplova, T.B. and A.S. Samerkhanova, 2006. The trend of the use of solid high-strength materials in microelectronics, medicine and jewelry. M.: GIAB, (10).
2. Darkovsky, Y., 2009. Automation of the sapphire single crystals production process by Kyropoulos method. Equipment and technology of crystal growth. I-st International Workshop, Bryansk.
3. Bradsky, G. and A. Kaehler, 2008. Learning OpenCV, O'Reilly. p. 1, ISBN 978-0-596-51613-0
4. Baghdasarov, H. S., L.A. Gorjainov, 2007. Heat and mass transfer during the single crystal growth by directional solidification. Moscow: FIZMALIT, 224p., ISBN 978-5-9221-0806-5
5. Lobatsevich, K.L., 2010. Improving of sapphire single crystals crystallization rate stability by Kyropoulos method by introduction of predictive control rate of single crystal mass change: the Dissertation for the degree of Candidate of Technical Sciences, Rybinsk, 141p.
6. Mark, S. Nixon and S. Alberto, 2008. Aguado. Feature Extraction and Image Processing. Academic Press, p. 88.
7. Huang, Z.K., et al., 2008. A New Image Thresholding Method Based on Gaussian Mixture Model. Applied Mathematics and Computation 205 (2): 899-907.
8. Taormina, R., et al., 2012. Artificial Neural Network simulation of hourly groundwater levels in a coastal aquifer system of the Venice lagoon. Engineering Applications of Artificial Intelligence 25 (8): 1670-1676.
9. Wu, C.L., et al., 2009. Predicting monthly streamflow using data-driven models coupled with data-preprocessing techniques. Water Resources Research 45. DOI:10.1029/2007WR006737.
10. Zhang, J., et al., 2009. Multilayer Ensemble Pruning via Novel Multi-sub-swarm Particle Swarm Optimization. Journal of Universal Computer Science 15 (4): 840-858.
11. Cheng, C.T., et al., 2005. Long-term prediction of discharges in Manwan Reservoir using artificial neural network models. Lecture Notes in Computer Science 3498: 1040-1045.

12. Chau, K.W., 2007. Application of a PSO-based neural network in analysis of outcomes of construction claims. Automation in Construction 16 (5): 642-646.

13. Trubaev, P.A., 2007. Analysis of high power technology processes and devices silicate material production. Bulletin of BSTU named after V.G. Shukhov, 1: 11-13.